DOI: 10.61782/fa.2023.0437

forum acusticum 2023

ENERGY RELATIONSHIPS IN ENCLOSURES

Jean-Dominique Polack[1*]
[1] Institut D'Alembert, Sorbonne Université/CNRS UMR 7190, Paris, France

ABSTRACT

This paper revisits the concept of active and reactive energies and their conservations. Conservation of active energy is expressed by the divergence of the stress-energy tensor, which is null outside sources. However, kinetic and potential energy are generally not equal, the difference being proportional to the average total curvature of the wave fronts: it vanishes in the case of plane waves. On the other hand, kinetic energy can always be diagonalized. As for the reactive energy, it is carried by the reactive intensity and a cross-energy which satisfy Maxwell's equations; conservation equations can be derived for their flux, which generalize both Poynting's theorem and the stress-energy tensor. The paper demonstrates some of these properties on simulated sound fields, on actual sound fields measured with an Ambisonics probe, and near the boundaries of an enclosure. An application to architectural acoustics simulation is also presented..

Keywords: *energy relations, stress-energy tensor, reactive energy, conservation equations.*

1. INTRODUCTION

This paper is a first step toward the derivation of a complete formulation for the conservation of energy in linear acoustics. It makes use of the conservation of the stress-energy tensor, that is, the covariance of the stress-energy tensor is null in linear acoustics, as first proven by P.M. Morse and K.U. Ingard [1]. At stake is a novel approach to sound field computation that naturally accounts for losses, whereas current computational methods for room acoustics do not, despite recent development in numerical acoustics such as [2].
Beside its derivation by Morse and Ingard [1], we know of only two attempts to apply this formalism to acoustics [2,4]. Some related ideas can be found in earlier papers from Stanzial [5] and Mann et al. [6]

2. NOTATIONS

We consider a 4-dimensional flat time-space with the diagonal Minkowski metric tensor η_{ij} and the volume element $dV=cdx^0...dx^3$ where x^0 is the time variable. The infinitesimal distance element is given by:

$$ds^2 = \eta_{ij} dx^i dx^j \tag{1}$$

where only the diagonal elements of η_{ij} are non null, with $\eta_{00} = -c^2$ and $\eta_{ii} = 1$ for $i > 0$. With Einstein's summation notation, the wave equation is then:

$$\Box \Phi = \nabla_i \eta^{ij} \partial_j \Phi \tag{2}$$

where $\Box$ is the Dalembertian operator, Φ is the velocity potential and η^{ij} the inverse matrix of η_{ij}. Note that ∇_i is the covariant derivation with respect to x^i, which for the Minkowski metric does not differ from the usual partial derivation ∂_i. Like ordinary differentiations, covariant derivations therefore commute in this specific metric. Note that by construction, all covariant derivatives of the elements of the metric tensor are null. In other words, the contravariant derivation ∇^i is defined by:

$$\nabla^i = \eta^{ij} \nabla_j = \nabla_j \eta^{ij} \tag{3}$$

One calls vectors tensors with one upper index, such as X^i; and covectors tensors with one lower index, such as $\Phi_i = \partial_i \Phi$.

3. MATHEMATICAL DERIVATIONS

[*] ***Corresponding author***: *jean-dominique.polack@sorbonne-universite.fr.*

3.1 Volume deformation

In general, the velocity potential Φ is a complex function. So one can consider the product $\Phi^*\Box\Phi$, where Φ^* is the complex conjugate of Φ. Differentiation rules lead to:

$$\Phi^*\Box\Phi = \Phi^*\nabla_i\eta^{ij}\partial_j\Phi = \nabla_i\eta^{ij}\left[\Phi^*\partial_j\Phi\right] - \partial_i\Phi^*\eta^{ij}\partial_j\Phi = 0 \quad (4)$$

that is, to:

$$\nabla_i\eta^{ij}\left[\Phi^*\partial_j\Phi\right] = \left[\partial_i\Phi^*\right]\eta^{ij}\partial_j\Phi \quad (5)$$

As the right member of the preceding equation is real, separating the real and imaginary parts leads to:

$$\nabla_i\left[\eta^{ij}\frac{\Phi^*\partial_j\Phi + \Phi\partial_j\Phi^*}{2}\right] = \partial_i\Phi^*\eta^{ij}\partial_j\Phi = 2L \quad (6)$$

for the real part, where L is the Lagrangian; and for the imaginary part, to:

$$\nabla_i\left[\eta^{ij}\frac{\Phi^*\partial_j\Phi - \Phi\partial_j\Phi^*}{2}\right] = \nabla^i\frac{\Phi^*\partial_j\Phi - \Phi\partial_j\Phi^*}{2} = 0 \quad (7)$$

It should be noticed that the term in brackets on the left hand side of Eqn. (6) can be rewritten as:

$$\eta^{ij}\frac{\Phi^*\partial_j\Phi + \Phi\partial_j\Phi^*}{2} = \eta^{ij}\partial_j\left(\tfrac{1}{2}|\Phi|^2\right) \quad (8)$$

that is, as the 4-gradient of a real function. As a consequence, it can be assimilated to a 4-velocity $\boldsymbol{V}^i$. Thus the real part of Eqn. (5) simply reduces to:

$$\nabla_i\boldsymbol{V}^i = 2L \quad (9)$$

meaning that the Lagrangian L amounts to a volume deformation (divergence of a velocity). Indeed, direct computation of the Lagrangian for spherical and cylindrical waves shows it is proportional to the average total curvature of the wave fronts

In a similar fashion, the imaginary part can be assimilated to a "covector" potential $\boldsymbol{A}_i$ with the gauge relation:

$$\nabla^i\boldsymbol{A}_i = 0 \quad (10)$$

3.2 Stress-energy tensor conservation

We now consider the product $\partial_k\Phi^*\Box\Phi$ Once more, differentiation rules lead to:

$$\begin{aligned}\partial_k\Phi^*\Box\Phi &= \partial_k\Phi^*\nabla_i\eta^{ij}\partial_j\Phi \\ &= \nabla_i\eta^{ij}\left[\partial_k\Phi^*\partial_j\Phi\right] - \left[\nabla_i\partial_k\Phi^*\right]\eta^{ij}\partial_j\Phi \\ &= \nabla_i\eta^{ij}\left[\partial_k\Phi^*\partial_j\Phi\right] - \left[\nabla_k\partial_i\Phi^*\right]\eta^{ij}\partial_j\Phi \\ &= \nabla^j\left[\partial_k\Phi^*\partial_j\Phi\right] - \left[\nabla_k\partial_i\Phi^*\right]\eta^{ij}\partial_j\Phi = 0\end{aligned} \quad (11)$$

As i and j are mute indices, separating the real and imaginary parts of the preceding equation leads to:

- for the real part:

$$\nabla^j\left[\partial_j\Phi^*\partial_k\Phi + \partial_j\Phi\partial_k\Phi^*\right] = \nabla_k\left[\partial_i\Phi^*\eta^{ij}\partial_j\Phi\right] \quad (12)$$

that is, to:

$$\nabla^i T_{ij} = 0 \quad (13)$$

where T_{ij} is the *symmetrical* stress-energy tensor, defined by:

$$T_{ij} = \frac{\partial_i\Phi^*\partial_j\Phi + \partial_i\Phi\partial_j\Phi^*}{2} - \frac{1}{2}\eta_{ij}\left(\partial_k\Phi^*\eta^{kl}\partial_l\Phi\right) \quad (14)$$

- for the imaginary part:

$$\begin{aligned}&\nabla^j\left[\partial_j\Phi^*\partial_k\Phi - \partial_j\Phi\partial_k\Phi^*\right] \\ &= \left[\nabla_k\partial_i\Phi^*\right]\eta^{ij}\partial_j\Phi - \left[\nabla_k\partial_i\Phi\right]\eta^{ij}\partial_j\Phi^* \\ &= -4\pi\,\mathrm{i}\,\boldsymbol{j}_k\end{aligned} \quad (15)$$

The convector $\boldsymbol{j}_k$ can be assimilated to a 4-current, as will become evident in next Section.

It is easy to recognise that the equation for the real part corresponds to the contravariant conservation of the stress-energy tensor. In acoustics, the different coefficients of the stress-energy tensor can be interpreted as [1]:

- the total energy density T_{00};
- the *active* acoustic intensity $\boldsymbol{I}$, proportional to T_{a0} and T_{0a}, where a takes the values 1, 2 or 3:

$$T_{a0} = T_{0a} = -c\boldsymbol{I}_a \quad (16)$$

- the symmetrical wave-stress tensor T_{ab}, where a and b take the values 1, 2 or 3.

Conservation of the stress-energy tensor T_{ij} therefore amounts to the conservation of *active* energy.

3.3 Maxwell's equations

On the other hand, let us introduce the antisymmetric tensor F_{ij} defined by:

$$F_{ij} = \nabla_i\boldsymbol{A}_j - \nabla_j\boldsymbol{A}_i = -F_{ji} \quad (17)$$

In other words, F_{ij} is the external differential form (curl) of the covector potential $\boldsymbol{A}_i$. Simple derivations lead to:

$$\begin{aligned}\nabla_i\boldsymbol{A}_j &= \nabla_i\frac{\Phi^*\partial_j\Phi - \Phi\partial_j\Phi^*}{2} \\ &= \frac{1}{2\mathrm{i}}\left(\partial_i\Phi^*\partial_j\Phi + \Phi^*\nabla_i\partial_j\Phi - \partial_i\Phi\partial_j\Phi^* - \Phi\nabla_i\partial_j\Phi^*\right)\end{aligned} \quad (18)$$

$$\nabla_j\boldsymbol{A}_i = \frac{1}{2\mathrm{i}}\left(-\partial_j\Phi^*\partial_j\Phi + \Phi^*\nabla_j\partial_i\Phi + \partial_j\Phi\partial_i\Phi^* - \Phi\nabla_j\partial_i\Phi^*\right) \quad (19)$$

and by subtracting the two equations, to:

$$F_{ij} = \nabla_i\boldsymbol{A}_j - \nabla_j\boldsymbol{A}_i = \frac{\partial_i\Phi^*\partial_j\Phi - \partial_j\Phi^*\partial_i\Phi}{2\mathrm{i}} \quad (20)$$

Due to its definition, F_{ij} naturally satisfies the Maxwell equations:

$$\begin{aligned}\nabla^i F_{ij} &= -2\pi\boldsymbol{j}_j \\ \nabla_{[k}F_{ij]} &= \nabla_k F_{ij} + \nabla_i F_{jk} + \nabla_j F_{ki} = 0\end{aligned} \quad (21)$$

where the square brackets indicate sum over all cyclic permutations, that is, anti-symmetrization. The first equation is nothing else but Eqn. (15), and leads to assimilate the convector $\boldsymbol{j}_k$ to a 4-current. The second

equation simply derives from the definition of tensor F_{ij} and the commutative property of covariant derivations. Indeed:

$$\nabla_{[k}F_{ij]} = \nabla_k\left[\nabla_i \boldsymbol{A}_j - \nabla_j \boldsymbol{A}_i\right] + \nabla_i\left[\nabla_j \boldsymbol{A}_k - \nabla_k \boldsymbol{A}_j\right] + \nabla_j\left[\nabla_k \boldsymbol{A}_i - \nabla_i \boldsymbol{A}_k\right] = 0 \quad (22)$$

Note that the first Eqn. (21) implies current conservation. Indeed, form the definition of $\boldsymbol{j}_i$:

$$\boldsymbol{j}_i = \frac{\nabla_i\partial_k\Phi\eta^{kl}\partial_l\Phi^* - \nabla_i\partial_k\Phi^*\eta^{kl}\partial_l\Phi}{4\pi\,\mathrm{i}} = \frac{1}{4\pi}\Im\left\{\left[\nabla_i\partial_k\Phi\right]\eta^{kl}\partial_l\Phi^*\right\} \quad (23)$$

we obtain:

$$\begin{aligned}\nabla^i\boldsymbol{j}_i &= \nabla_j\eta^{ji}\frac{\nabla_i\partial_k\Phi\eta^{kl}\partial_l\Phi^* - \nabla_i\partial_k\Phi^*\eta^{kl}\partial_l\Phi}{4\pi\,\mathrm{i}}\\ &= \frac{1}{4\pi\,\mathrm{i}}\left[\nabla_j\eta^{ji}\nabla_i\partial_k\Phi\eta^{kl}\partial_l\Phi^* + \nabla_i\partial_k\Phi\eta^{kl}\eta^{ij}\nabla_j\partial_l\Phi^*\right]\\ &\quad -\frac{1}{4\pi\,\mathrm{i}}\left[\nabla_j\eta^{ji}\nabla_i\partial_k\Phi^*\eta^{kl}\partial_l\Phi + \nabla_i\partial_k\Phi^*\eta^{kl}\eta^{ij}\nabla_j\partial_l\Phi\right]\\ &= \frac{1}{4\pi\,\mathrm{i}}\left[\nabla_j\eta^{ji}\nabla_i\partial_k\Phi\eta^{kl}\partial_l\Phi^* - \nabla_j\eta^{ji}\nabla_i\partial_k\Phi^*\eta^{kl}\partial_l\Phi\right]\\ &= \frac{1}{4\pi\,\mathrm{i}}\left[\nabla_j\eta^{ji}\nabla_k\partial_l\Phi\eta^{kl}\partial_l\Phi^* - \nabla_j\eta^{ji}\nabla_k\partial_i\Phi^*\eta^{kl}\partial_l\Phi\right]\end{aligned} \quad (24)$$

The commutation relations for covariant derivatives leads to:

$$\nabla_j\nabla_k\eta^{ji}\partial_i\Phi = \nabla_k\left[\nabla_i\eta^{ji}\partial_i\Phi\right] \quad (25)$$

where we recognize in the right hand side the generalized wave equation Eqn. (2). The term is therefore equal to 0. Thus:

$$\nabla_j\eta^{ji}\nabla_k\partial_i\Phi\eta^{kl}\partial_l\Phi^* = \nabla_j\eta^{ji}\nabla_k\partial_i\Phi^*\eta^{kl}\partial_l\Phi = 0 \quad (26)$$

and Eqn. (24) becomes:

$$\nabla^i\boldsymbol{j}_i = 0 \quad (27)$$

There remains to interpret the antisymmetric tensor F_{ij} in acoustical terms. By comparison with the stress-energy tensor, it is obvious that $F_{a0} = -F_{0a}$, where a takes the values 1, 2 or 3, is the *reactive* acoustic intensity covector $\boldsymbol{Q}_i$. Therefore, by analogy, we call the terms $F_{ab} = -F_{ba}$, where a and b take the values 1, 2 or 3, the *reactive* wave stress. We then retrieve the usual form of Maxwell's equations by introducing a reactive stress covector $\boldsymbol{B}_i$, defined by:

$$\boldsymbol{B}_a = F_{bc} \quad (28)$$

where *a, b* and *c* respectively take the value *1, 2* and *3* and their cyclic permutations. With these notations, the Maxwell equations Eqn. (20) take their usual form:

$$\nabla^i\boldsymbol{Q}_i + 2\pi\boldsymbol{j}_0 = 0 \quad \nabla^0\boldsymbol{Q}_a + \mathrm{Curl}\left(\boldsymbol{B}\right)_a + 2\pi\boldsymbol{j}_a = 0 \quad \nabla_i\boldsymbol{B}_i = 0 \quad \nabla_0\boldsymbol{B}_a + \mathrm{Curl}\left(\boldsymbol{Q}\right)_a = 0 \quad (29)$$

3.4 Conservation of reactive energy

By analogy with electromagnetic waves, the stress-energy tensor for the reactive energy can be written as [5]:

$$\hat{T}_{ij} = \left[F_{ik}F_{jl}\eta^{kl} - \frac{1}{4}\eta_{ij}F_{kl}F_{mn}\eta^{km}\eta^{ln}\right] \quad (30)$$

In term of reactive intensity and stress, we obtain:

$$\begin{aligned}\hat{T}_{00} &= \frac{c^2}{2}\left[\boldsymbol{Q}^2 + \boldsymbol{B}^2\right]\\ \hat{T}_{0a} &= c\boldsymbol{S}_a = \hat{T}_{a0},\ a = 1,2,3 \quad \text{with} \quad \boldsymbol{S} = \boldsymbol{Q}\wedge\boldsymbol{B}\\ \hat{T}_{ab} &= -\left(\boldsymbol{Q}_a\boldsymbol{Q}_b + \boldsymbol{B}_a\boldsymbol{B}_b\right) + \frac{1}{2}\left[\boldsymbol{Q}^2 + \boldsymbol{B}^2\right]\delta_{ab}\end{aligned} \quad (31)$$

where δ_{ab} is the Kronecker symbol and $\boldsymbol{S}$ the Pointing vector, and with the conservation law:

$$\nabla^i\hat{T}_{ij} = F_{jk}\boldsymbol{j}^k \quad (32)$$

3.5 In summary

We have proven that, if $\boldsymbol{\Phi}$ is a velocity potential satisfying the wave equation:

- the associated Lagrangian (Eqn. 6) is the divergence of some 4-vector $\boldsymbol{V}^i$, as is well known from theory [8];
- the associated stress-energy tensor (Eqn. 14) is conserved (vanishing divergence, Eqn. 13);
- the imaginary parts of the intensity and wave-stress tensor satisfy Maxwell's equations (Eqn. 20 and 29), and build a reactive stress-energy tensor (Eqn. 31).

To the best of our knowledge, the last result is new.

4. SOME PRELIMINARY EXAMPLES

We are presently adapting OpenMIDAS, the Matlab version of the MIDAS software package [9,10], to the processing of the 4 channels of Ambisonics microphones. Therefore, the results presented here are preliminary and do not cover all aspects of the theory yet.

Note that Ambisonics measurements can only deliver information about the structure of the stress-energy tensor. Verifying its conservation needs specific probes that we have already designed [11]. There remain to calibrate them and develop the specific measurement procedure.

4.1 FVTD simulation of a hallway

Fig. 1 presents the hallway that Meacham et al. [12] simulated with a Finite Volume Time Difference numerical scheme [2]. It includes many lateral alcoves that diffuse sound. The scheme incorporates by design the conservation of energy, that is, it intrinsically satisfies Eqn. (13) for the first coordinate. We have derived the numerical equivalents for the conservation of intensity (last three coordinates), but have not implemented it in the scheme yet.

Figure 1. The hallway at Institut D'Alembert, Paris.

Fig. 2 presents broad-band simulation results for the stress-energy tensor, defined by Eqn. (14), obtained in one "passage" where the hallways narrows, as can be seen in Fig. 1. The three major peaks in energy correspond resp. to the direct sound and two reflected waves at the ends of the hallway. As expected, the sound intensity T_{01} along the length of the hallway changes sign at each reflections.

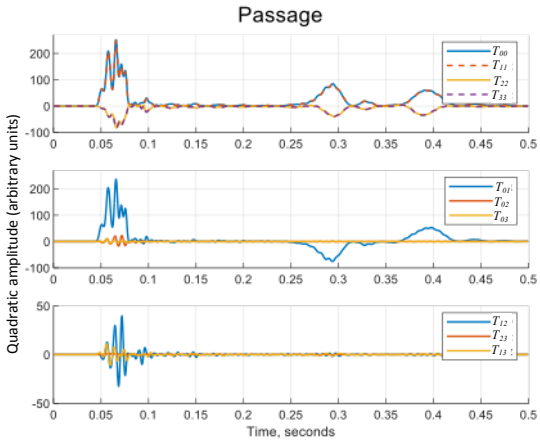

Figure 2. Components of the stress-energy tensor computed in the hallway (from [12]).

The relative agreement between T_{00} and T_{11} implies that most of the energy density in the hallway is driven by the longitudinal component along x^1. To the contrary, the T_{22} and T_{33} terms, resp. transversal and vertical components, are also grouped fairly closely, and for the most part, oppose the motion of the energy density. This implies that kinetic energy dominates. As a consequence, the Lagrangian L is strictly positive, indicating that diffraction takes place in the hallways. Indeed, the Lagrangian of cylindrical or spherical waves are strictly positive (see Sect. 3.1).

All of the off-diagonal terms of the wave-stress tensor T_{ab} are non-zero, but are nonetheless much smaller in magnitude than the diagonal terms. There remains to diagonalize the wave-stress tensor, which was not attempted in [12].

We observed other patterns in other sections of the hallway, especially in the lateral alcoves where the T_{22} and T_{33} terms become positive, indicating a dominating potential energy. No satisfactory explanation for it has been found so far.

We hope to soon correlate simulation with measurements in the same hallway.

4.2 Measurements in front of scattering surfaces

In 2017, we carried out absorption and scattering measurements [11] on wall elements at the Experimental Media and Performing Arts Center (EMPAC) of the Rensselaer Polytechnic Institute (Troy, NY, US).

Figure 3. Scattering wall at EMPAC.

Fig. 3 presents the setup, with an Ambisonic microphone located very close to the wall. The source was located, either within the room on the normal to the wall at the position of the microphone; or close to the wall for measurements at grazing incidence.

Fig. 4 presents the T_{00} and T_{01} terms of the stress-energy tensor when sound impinges on the surface at normal incidence along x^1 (source within the room).

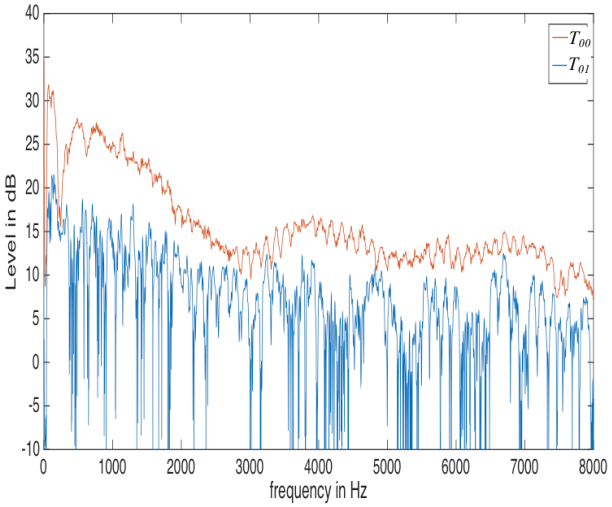

Figure 4. Scattering wall at EMPAC.

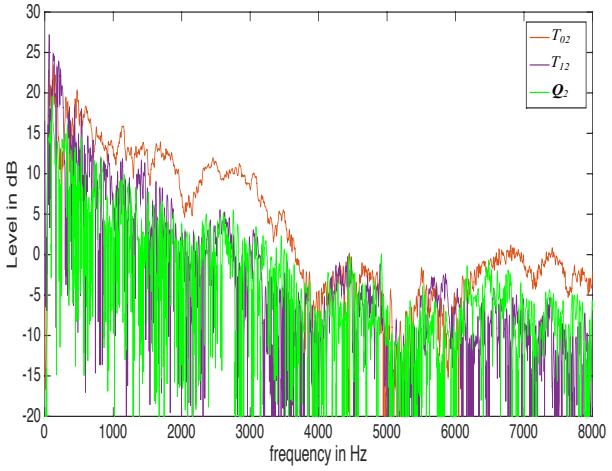

Figure 5. Scattering wall at EMPAC.

One sees in Fig. 4 that the active sound intensity T_{01} is smaller than the total energy T_{00} at all frequencies, as is expected since their ratio is equal to sound absorption, always smaller than 1. In the present case, the ration is much smaller than 1, except at very low frequencies where there is no signal, in accordance with a scattering surface of low absorption.

Fig. 5 presents the T_{02} and T_{12} terms of the stress-energy tensor when sound impinges on the surface at grazing incidence along x^2 (source close to the wall). It also presents the grazing reactive intensity $\boldsymbol{Q}_2$.
One sees in Fig. 5 that the grazing sound intensity T_{02} is larger than both the T_{12} component of the wave-stress tensor and the grazing reactive intensity $\boldsymbol{Q}_2$, except at some single frequencies. On the other hand, the reactive intensity has the same magnitude as T_{12}, indicating the persistence of a reactive field. More measurements are needed to understand this reactive field.

4.3 Direct computation of stress-energy tensor

The stress-energy tensor formalism has already been used to describe specific sound fields. In [4], direct computation of its components was achieved under supplementary hypotheses, similar to the constitutional laws of continuum mechanics. The corresponding boundary conditions include absorption linking total energy and intensity, and a new boundary condition that redistribute intensity in different directions (scattering).

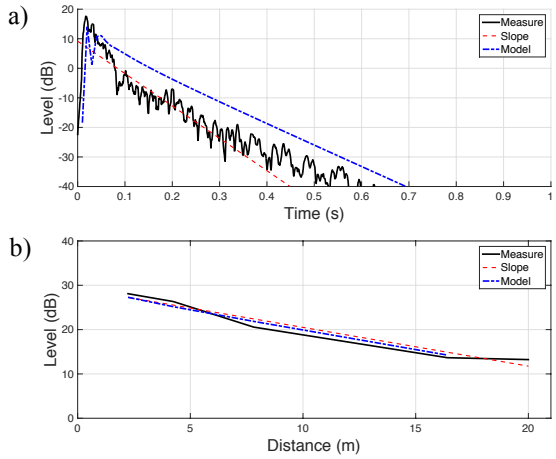

Figure 6. Comparison of model with time (a) and space (b) decays for an open-space office (from [4]).

Fig. 6 presents a comparison of the model with actual decay measurements in a large open-space office. The time decay is calculated and measured for an Ambisonics receiver located at 4 m from the omnidirectional dodecahedral sound source (pressure signals only). With adapted values of absorption and scattering coefficients, the agreement is rather correct, except that the model does not properly reproduce the

early sound within the first 100 ms of the time decay. On the other hand, the space decay is correctly predicted.
Presently, the challenge concerns the prediction and measurement of scattering coefficient, which remains an ongoing project (see Sect. 4.2).

5. CONCLUSION

The present paper is a first attempt to present a comprehensive view of energy relationships in enclosures. Beyond a complete and detailed derivation of the stress-energy tensor, that sums up most of the energetic quantities associated with a sound field, it presents partial analysis of simulations and measurements that illustrate the structure of the stress-energy tensor. There remains to experimentally verify the conservation of the stress-energy tensor, and predict scattering coefficients for direct computation of stress-energy tensors, which needs further developments.
More experimental results will be presented at the conference when the upgrading of OpenMIDAS is complete, based on the many Ambisonics measurements of concert halls that the author has collected over the years.

6. ACKNOWLEDGMENTS

The author thanks Aidan Meacham for his contribution to Sect. 4.1, and Bai Xin for his contribution to Sect. 4.2.

7. REFERENCES

[1] P.M. Morse and K.U. Ingard: *Theoretical Acoustics*. New York : Mc Graw-Hill Book Company, 1968

[2] S. Bilbao, B. Hamilton, J. Botts, and L. Savioja, "Finite Volume Time Domain Room Acoustics Simulation under General Impedance Boundary Conditions", *IEEE Trans. ALSP*, vol. 24, no 1, pp. 161–173, 2016.

[3] D. Stanzial, D. Bonzi, and G. Schiffrer, "Four-dimensional treatment of linear acoustic fields and radiation pressure", *Acta Ac. u. Acustica.*, vol. 88, pp. 213–224, 2992

[4] H. Dujourdy, B. Pialot, T. Toulemonde, and J.D. Polack, "An energetic wave equation for modelling diffuse sound fields - Application to open offices", *Wave Motion*, vol. 87, pp. 193–212, 2019.

[5] D. Stanzial and C.E. Graffigna, "On the general connection between wave impedance and complex sound intensity", *Proc. Mtgs. Acoust.*, vol. 30, 055013, 2017; doi: 10.1121/2.0000797

[6] J.A. Mann, J. Tichy, and A.J. Romano, "Instantaneous and time-averaged energy transfer in acoustic fields", *J. Aoust. Soc. Am.*, vol. 82, no. 1, pp. 17–30, 1987

[7] F. Debbasch: "What is a mean gravitational field?", *Eur. Phys. J. B*, vol.37, pp. 257–269, 2004

[8] P.J. Olver: *Application of Lie Groups to Differential Equations (2nd Edition)*. New York : Springer-Verlag, 1993 ; pp. 247.

[9] J.D. Polack, A.H. Marshall, and G. Dodd: "Digital evaluation of the acoustics of small models: the MIDAS package", *J. Acoust. Soc. Am.*, vol.85, pp. 185–193, 1989.

[10] G. Defrance: "Caractérisation du mélange dans les réponses impulsionnelles de salles. Application à la détermination expérimentale du temps de mélange". Paris: Doctoral Thesis, UPMC, 2009.

[11] J.D. Polack, H. Dujourdy, N. Xiang, and X. Bai: "Novel scattering coefficient for diffusely reflecting surfaces", *ASA 174th Meeting*, (New Orleans, USA), 2017.

[12] A. Meacham, R. Badeau, and J.D. Polack: "Confirming dimensional reduction assumptions for the energy-stress tensor through comparison with high-frequency wave-based pressure simulations", *16th CFA*, (Marseille, France), paper 254, 2022.